Expression of Multidrug Resistance Protein and Messenger RNA Correlate with ^{99m}Tc-MIBI Imaging in Patients with Lung Cancer

Jinshan Zhou, Kotaro Higashi, Yoshimichi Ueda, Yuko Kodama, Dachuan Guo, Fumiko Jisaki, Aya Sakurai, Tsutomu Takegami, Shogo Katsuda, and Itaru Yamamoto

Departments of Radiology and Pathology and Division of Tropical Medicine, Medical Research Institute, Kanazawa Medical University, Ishikawa, Japan

In vitro studies have shown that ^{99m}Tc-sestamibi (MIBI) is a transport substrate for the P-glycoprotein (Pgp) pump and the multidrug resistance–associated protein (MRP) pump. However, whether MRP and lung resistance protein (LRP) affect tumor accumulation and efflux of ^{99m}Tc-MIBI in lung cancer is not known. In this study, we explored whether Pgp and the other pumps, MRP and LRP, affect tumor accumulation and efflux of ^{99m}Tc-MIBI in lung cancer. **Methods:** Thirty-four lung cancer patients who underwent surgery were examined. Before surgery, ^{99m}Tc-MIBI SPECT was performed 15 min and 180 min after injection, and early uptake, delayed uptake (L/Nd), and washout rate (L/Nwr) of ^{99m}Tc-MIBI were obtained. Pgp, MRP, and LRP expression were investigated by immunohistochemistry. The messenger RNA (mRNA) level of Pgp, MRP, and LRP was determined by real-time reverse-transcription polymerase chain reaction. The lung cancer ^{99m}Tc-MIBI images were correlated with protein and mRNA expression. **Results:** The mean L/Nd of the Pgp (−) group was significantly higher than that of the Pgp (++) group ($P = 0.0324$). The Pgp (++) group had a higher L/Nwr than did the Pgp (−) group ($P = 0.0269$). The mean L/Nd of the Pgp mRNA low-expression group was significantly higher than that of the Pgp mRNA high-expression group ($P = 0.0127$). The Pgp mRNA high-expression group had a higher L/Nwr than did the Pgp mRNA low-expression group ($P = 0.0825$). No appreciable correlation was found between the lung cancer ^{99m}Tc-MIBI images and the expression of MRP or LRP on the level of protein or mRNA. **Conclusion:** These data suggest that an increased level of Pgp expression correlates with a low accumulation on delayed scans and a high L/Nwr of ^{99m}Tc-MIBI in lung cancer. Neither MRP nor LRP expression on the level of either protein or mRNA correlated significantly with tumor accumulation or efflux of ^{99m}Tc-MIBI in lung cancer.

Key Words: ^{99m}Tc-methoxyisobutylisonitrile; lung cancer; P-glycoprotein; multidrug resistance–associated protein; lung resistance protein

J Nucl Med 2001; 42:1476–1483

Multidrug resistance (MDR) is the main barrier to efficient chemotherapy of cancer. MDR has been closely associated with altered expression of MDR phenotype, and in lung cancer the MDR phenotype has been defined on the basis of the cellular drug targets involved, that is, P-glycoprotein (Pgp), MDR-associated protein (MRP), lung resistance protein (LRP), and atypical MDR (mediated through altered expression of topoisomerase type II) (*1–4*). In contrast to other types of MDR, pure atypical MDR is not associated with alterations in drug accumulation or retention (*5*). Pgp, encoded by the MDR1 gene, is a 170-kDa transmembrane glycoprotein and acts as an adenosine triphosphate (ATP)–driven drug efflux pump to reduce drug accumulation (*6*). MRP is a 190-kDa membrane-bound glycoprotein and can act as a glutathione S-conjugate efflux pump by transporting drugs that are conjugated or cotransported with glutathione (*7,8*). Both Pgp and MRP are integral membrane proteins belonging to the ATP-binding cassette (ABC) superfamily of transporter proteins, which appear to confer resistance by decreasing intracellular drug accumulation and enhancing drug efflux (*9,10*). In contrast, LRP is not an ABC transporter protein. LRP has recently been identified as a vault protein, which is a typical multisubunit structure involved in nucleocytoplasmic transport (*11*). Determination of these MDR proteins at the time of diagnosis is imperative to the development of rational therapeutic strategies for preventing drug resistance.

Nuclear medicine techniques, such as SPECT, that rely on biochemical and physiologic characteristics of the tumor have been used to evaluate the MDR phenotype. ^{99m}Tc-sestamibi (MIBI), a member of the isonitrile class of coordination compounds (*12*), is a lipophilic cation approved for clinical use as a myocardial perfusion imaging agent (*13*). ^{99m}Tc-MIBI has been reported to be useful for the detection of a variety of tumors, including lung cancer (*14–17*). ^{99m}Tc-MIBI, in addition to other drugs, has also been reported to be washed out from cells by a Pgp efflux pump (*18*). The potential advantage of ^{99m}Tc-MIBI imaging lies in its superiority in noninvasively detecting the presence of

Received Mar. 1, 2001; revision accepted Jun. 12, 2001.

For correspondence or reprints contact: Kotaro Higashi, MD, Department of Radiology, Kanazawa Medical University, 1-1, Daigaku, Uchinada, Kahoku-gun, Ishikawa, 920-0293, Japan.

Pgp overexpression in vivo (*19–21*). Recently, ^{99m}Tc-MIBI efflux was shown to be a substrate for MRP in vitro (*22*). However, whether MRP and LRP affect tumor accumulation and efflux of ^{99m}Tc-MIBI in lung cancer is not known. The aim of this study was to determine whether Pgp and the other pumps, MRP and LRP, affect tumor accumulation and efflux of ^{99m}Tc-MIBI in lung cancer.

MATERIALS AND METHODS

Patients

Thirty-four patients (8 women, 26 men; age range, 37–82 y; mean age ± SD, 69.1 ± 8.9 y) with histologically confirmed lung cancer were included in the study. Twenty-two patients had adenocarcinoma, 5 had squamous cell carcinoma, 2 had small cell carcinoma, 2 had adenosquamous cell carcinoma, 1 had large cell carcinoma, and 2 had metastatic lung tumors. None had received prior treatment, including chemotherapy, radiotherapy, and surgery. All patients underwent ^{99m}Tc-MIBI SPECT followed by surgery. All tumor samples were analyzed by immunohistochemistry, and 10 samples were analyzed by reverse-transcription (RT) polymerase chain reaction (PCR).

^{99m}Tc-MIBI Chest Imaging

Chest imaging was performed with a double-head gamma camera equipped with a high-resolution parallel-hole collimator (PRISM 2000; Marconi Medical Systems, Cleveland, OH). Images were obtained 15 and 180 min after the injection of 740 MBq ^{99m}Tc-MIBI. Early and delayed SPECT of the chest was performed on all patients. For SPECT of the chest, 72 projections were obtained using a 64 × 64 matrix at 45 s per view. Image reconstruction was performed using filtered backprojection with Butterworth and ramp filters. Transverse, coronal, and sagittal sections were reconstructed. Attenuation correction was not applied.

SPECT images were compared with chest CT images, and accumulation in lung tumors was interpreted by 2 nuclear medicine physicians. The findings on the ^{99m}Tc-MIBI chest images were evaluated semiquantitatively. Regions of interest (ROIs) were manually defined on the transaxial tomograms that showed the lesion's highest uptake to be in the middle of the tumor. The ROIs placed on the lesions (L) encompassed all pixels that had uptake values of >90% of the maximum uptake in that slice, and the average counting rate in each ROI was calculated. Another ROI of the same size was then drawn over the contralateral normal lung (N) on the same transverse section. The early uptake (L/Ne) and the delayed uptake (L/Nd) were obtained. The washout rate (L/Nwr) was calculated using the following formula: L/Nwr = (L/Ne − L/Nd) × 100/(L/Ne).

Immunohistochemistry

Expression of Pgp, MRP, and LRP was assessed by immunohistochemistry. The surgically resected tumors were routinely fixed in 10% formalin and embedded in paraffin. The largest section in the middle of the tumor was stained for immunohistochemical study, which was performed using a streptavidin–biotin complex. For immunostaining, the primary antibodies used were the mouse monoclonal antibody (mAb) against Pgp (JSB-1; Novocastra Laboratories Ltd., Newcastle, U.K.), the rabbit mAb against MRP (MRPr1; Nichirei Corp., Tokyo, Japan), and the mouse mAb against LRP (LRP-56; Nichirei Corp.). Sections 4 μm thick were cut from the formalin-fixed paraffin-embedded materials and treated with xylene to remove the wax. The endogenous peroxidase activity was blocked by incubation in 0.3% hydrogen peroxide in methanol. Nonspecific protein binding was inhibited by treatment with 10% normal serum for 10 min at 37°C, and the specimens were then incubated with JSB-1 (1:20), MRPr1 (1:10), or LRP-56 (1:10) overnight at 4°C. The slides were preincubated and rinsed in phosphate-buffered saline and then treated with the biotinylated secondary antibody and peroxidase-conjugated streptavidin. The final reaction product was revealed by exposure to 0.03% diaminobenzidine, and the nuclei were counterstained with Mayer's hematoxylin. For a negative control, appropriately diluted nonimmune sera were applied instead of the primary antibodies. Kidney tissue (proximal tubules) from a healthy adult human was used as a positive control for Pgp (*23*), and colon tissue (epithelium) from a healthy adult human was used as a positive control for both MRP and LRP (*24,25*). The results of immunostaining were independently interpreted by a pathologist who knew none of the clinical information. Immunostaining was examined in 10 high-power fields. The average percentage of the positive area was calculated for 10 fields for each of the tumors. Pgp, MRP, and LRP expression was graded according to the percentage of stained tumor cells as − (0%–9%), + (10%–69%), or ++ (70%–100%).

Quantitative RT PCR

Standard Preparation. The surgically resected tumor specimens were rapidly frozen in liquid nitrogen and stored at −70°C until processing. MDR1, MRP, and LRP transcripts were amplified by RT PCR and subcloned from patients known to carry the respective breakpoint. The cloned products were purified, and the identities of inserts were sequenced with ABI PRISM BigDye Terminators Cycle Sequencing Kit (a fluorescent sequencing ready reaction kit; Applied Biosystems, Foster City, CA). Plasmid DNA was serially diluted and ranged from 10:6 to 10:1 pg/μL. The glyceraldehyde-3-phosphate dehydrogenase (GAPDH) standard was provided in the TaqMan GAPDH Control Reagents kit (Applied Biosystems). GAPDH messenger RNA (mRNA) serial dilutions ranged from 80 to 50 ng/mL

Real-Time RT PCR. Expression of the target genes (MDR1, MRP, and LRP) and the endogenous reference GAPDH was quantified using the primers, probes, and standards. The primers and TaqMan probes were designed using the software Primer Express (Applied Biosystems) (Table 1). The RT PCR was performed according to a TaqMan 2-step method using an ABI PRISM 7700 Sequence Detection System (Applied Biosystems). The nontemplate controls, standard dilutions, and tumor samples were assayed. Total RNA was prepared from the frozen specimens. Total RNA (200 ng) isolated from tumor samples was reverse transcribed to complementary DNA (cDNA) using an oligo deoxythymidine primer. A 25-mm volume of PCR reaction mixture was used, containing 200 ng of the sample cDNA; TaqMan buffer; 200 mmol/L deoxy-ATP, deoxycytidine triphosphate, and deoxyguanosine triphosphate; 400 mmol/L deoxyuridine triphosphate; 5.5 mmol/L magnesium chloride; 0.025 U/mL AmpliTaq Gold DNA polymerase (Applied Biosystems); 0.01 U/mL AmpErase uracil *N*-glycosylase (Applied Biosystems); 200 nmol/L forward and reverse primers; and 100 nmol/L probe. The PCR cycling conditions included an initial phase of 2 min at 50°C, followed by 10 min at 95°C for AmpErase, 40 cycles of 15 s at 95°C, and 1 min at 60°C.

Quantification of the PCR products was based on the TaqMan 5′ nuclease assay (*26*) using the ABI PRISM 7700 Sequence Detec-

TABLE 1
Oligonucleotides Used for PCR Amplifications

Gene	Quantification method	Sequence	cDNA
MDR1	Forward primer	5′CCCAGGAGCCCATCCTGT3′	3774-3791
	Reverse primer	5′CCCGGCTGTTGTCTCCATA3′	3838-3821
	Probe	5′(FAM)TGACTGCAGCATTGCTGAGAACATTGC(TAMRA)3′	3793-3819
MRP	Forward primer	5′AAGCGCCTCGAGTCGGT3′	3617-3633
	Reverse primer	5′TCGAATGACGCTGACCCC3′	3694-3677
	Probe	5′(FAM)AGCCGCTCCCCGGTCTATTCCC(TAMRA)3′	3635-3656
LRP	Forward primer	5′TTTCGATGACTTCCATAAGAACTCA3′	1881-1905
	Reverse primer	5′TTCCGAGGTCTCAAAGCCAA3′	1950-1931
	Probe	5′(FAM)CCCGCATCATTCGCACTGCTGT(TAMRA)3′	1907-1928
GAPDH	Forward primer	5′GAAGGTGAAGGTCGGAGTCA3′	
	Reverse primer	5′GAAGATGGTGATGGGA3′	
	Probe	5′(JOE)CAAGCTTCCCGTTCTCAGCC(TAMRA)3′	

tion System. The starting quantity of a specific mRNA in an unknown sample was determined by preparing a standard curve using known dilutions of the standard cDNA. The standard curve was generated on the basis of the linear relationship between the Ct value (corresponding to the cycle number at which a significant increase in the fluorescence signal was first detected) and the logarithm of the starting quantity (*27*). The unknown samples were quantified by the software of the ABI PRISM 7700 Sequence Detector System, which calculated the Ct value for each sample and then determined the initial quantity of the target using the standard curve. The amount of the target was normalized to the GAPDH reference. In accord with our results for agarose electrophoresis, the limit for Pgp mRNA high expression was set at Pgp/GAPDH $>$ 0.03, the limit for MRP mRNA high expression was set at MRP/GAPDH $>$ 0.03, and the limit for LRP mRNA high expression was set at LRP/GAPDH $>$ 0.1.

Statistical Analysis. The results for L/Ne, L/Nd, and L/Nwr were expressed as mean ± 1 SD. The differences in L/Ne, L/Nd, and L/Nwr between patients with (−), (+), and (++) Pgp, MRP, or LRP expression were determined using an independent Student *t* test. The differences in L/Ne, L/Nd, and L/Nwr between patients with high and low Pgp mRNA, MRP mRNA, or LRP mRNA expression were determined using an independent Student *t* test. If *P* was $<$0.05, the difference was considered significant.

RESULTS

All 34 surgically obtained tissue samples were assessed to estimate the levels of Pgp, MRP, and LRP expression on protein level. Ten samples were analyzed to estimate the levels of Pgp, MRP, and LRP expression on mRNA level. Table 2 summarizes the immunohistochemical results and the RT PCR data.

Correlation of ^{99m}Tc-MIBI Results with Immunohistochemical Results

No correlation was found between L/Ne and the expression of Pgp, MRP, or LRP. The mean L/Nd (2.182 ± 1.165) of the Pgp (−) group was significantly higher than that (1.058 ± 0.143) of the Pgp (++) group ($P = 0.0324$) (Figs. 1, 2, and 3A). L/Nd was not related to the expression of MRP or LRP (Figs. 3B and 3C). The Pgp (++) group had a higher mean L/Nwr (40.68% ± 21.657%) than did the Pgp (−) group (−0.66% ± 35.066%, $P = 0.0269$) (Figs. 1, 2, and 4A). L/Nwr was not related to the expression of MRP or LRP (Figs. 4B and 4C).

Correlation of ^{99m}Tc-MIBI Results with RT PCR Results

No correlation was found between L/Ne and the level of Pgp mRNA, MRP mRNA, or LRP mRNA. The mean L/Nd (2.57 ± 0.731) of the Pgp mRNA low-expression group was significantly higher than that (1.318 ± 0.519) of the Pgp mRNA high-expression group ($P = 0.0127$) (Fig. 5A). L/Nd was not related to the level of MRP mRNA or LRP mRNA. Statistical support was found toward a significant difference in L/Nwr between the Pgp mRNA high-expression group (31.967% ± 44.447%) and the Pgp mRNA low-expression group (−21.450% ± 25.651%, $P = 0.0825$) (Fig. 5B). L/Nwr was not related to the level of MRP mRNA or LRP mRNA.

DISCUSSION

Evidence has shown that Pgp as a drug efflux pump extrudes ^{99m}Tc-MIBI and other drugs from cells and that Pgp expression and enhanced efflux of ^{99m}Tc-MIBI from these cells are closely connected (*18,22*). In animal models, faster clearance of ^{99m}Tc-MIBI is observed in tumors that express Pgp than in those that do not express Pgp (*3,18*). There have also been some reports about the clinical relevance of Pgp and ^{99m}Tc-MIBI. A study of untreated breast cancer patients showed that ^{99m}Tc-MIBI L/Nwr values from breast cancers overexpressing Pgp were 2.7 times higher than those from cancers not expressing Pgp (*21*). An inverse correlation between the tumor-to-background ratio of ^{99m}Tc-MIBI and the density of Pgp expression in the tumors of patients with breast and lung cancer has also been reported (*19*). Our clinical data revealed that the mean L/Nd of the Pgp (−) group was significantly higher than that of the Pgp (++) group ($P = 0.0324$) (Figs. 1, 2, and 3A). The Pgp (++) group had a higher L/Nwr than did the Pgp (−) group ($P = 0.0269$) (Figs. 1, 2, and 4A). No correlation was found

TABLE 2
Patient Characteristics and Radionuclide Imaging Results

Patient no.	Age (y)	Sex	Histology	Tumor size (cm)	^{99m}Tc-MIBI SPECT			Immunohistochemistry			RT PCR		
					L/Ne	L/Nd	L/Nwr (%)	Pgp	MRP	LRP	MDR1	MRP	LRP
1	73	M	ADE	2.8	3.81	1.00	73.8	++	++	+	0.5435	0.0028	0.0784
2	59	M	Meta	2.6	1.52	1.00	34.2	++	+	++	—	—	—
3	37	M	Large	7.0	2.18	1.35	38.1	++	+	+	—	—	—
4	62	F	ADE	2.2	1.77	1.00	43.5	++	+	++	—	—	—
5	72	F	ADE	1.9	1.16	1.00	13.8	++	−	++	—	—	—
6	56	M	ADE	1.0	1.00	1.00	NA	++	−	++	0.0707	0.0004	0.2489
7	60	M	ADE	5.5	1.00	1.00	NA	+	++	+	0.0914	0.1750	0.1643
8	70	M	Small	5.0	1.3	1.48	−13.8	+	++	+	—	—	—
9	82	M	ADE	3.4	2.15	3.18	−47.9	+	++	++	0.0035	0.0448	0.1035
10	74	M	ADE	3.2	1.93	2.58	−33.7	+	++	+	0.0019	0.0096	0.1386
11	74	M	ADE	2.7	1.88	1.70	9.6	+	+	+	0.0427	0.1623	0.0976
12	78	M	ADESQ	1.8	2.78	1.00	64.0	+	+	++	0.0489	0.0277	0.0236
13	64	F	ADE	1.6	1.78	1.00	43.8	+	+	++	—	—	—
14	66	M	ADE	2.5	1.85	2.21	−19.5	+	+	++	0.1082	0.0686	1.2370
15	58	M	ADE	1.5	1.00	1.00	NA	+	+	++	—	—	—
16	72	M	ADE	2.3	1.00	1.00	NA	+	+	+	—	—	—
17	72	M	Meta	1.5	1.00	1.00	NA	+	+	−	—	—	—
18	74	F	ADE	2.8	2.03	1.97	3.0	+	+	++	—	—	—
19	72	F	ADE	1.2	1.00	1.00	NA	+	−	++	—	—	—
20	58	F	ADE	2.8	1.00	1.00	NA	+	−	+	—	—	—
21	66	M	ADE	2.8	3.99	2.37	40.6	−	++	++	—	—	—
22	81	M	SCC	3.0	2.29	4.10	−79.0	−	+	+	—	—	—
23	72	M	ADE	2.1	1.61	1.97	−22.4	−	+	++	—	—	—
24	70	M	ADESQ	2.5	1.57	1.42	9.6	−	+	++	—	—	—
25	66	F	ADE	2.6	1.36	1.78	−30.9	−	+	+	—	—	—
26	78	M	ADE	4.0	1.33	1.54	−15.8	−	+	++	0.0027	0.0045	0.0125
27	73	M	SCC	2.7	2.09	1.45	30.0	−	+	+	—	—	—
28	76	M	ADE	4.0	3.37	2.98	11.6	−	+	−	0.0278	0.0283	0.0409
29	76	M	ADE	1.8	1.92	1.74	9.4	−	+	+	—	—	—
30	75	M	SCC	3.2	2.80	1.84	34.3	−	+	+	—	—	—
31	66	M	SCC	2.5	1.00	1.00	NA	−	+	−	—	—	—
32	79	M	Small	2.2	2.50	1.94	22.4	−	+	−	—	—	—
33	72	M	SCC	2.8	1.63	1.25	23.3	−	−	−	—	—	—
34	68	F	ADE	3.6	3.65	5.17	−41.6	−	−	++	—	—	—

ADE = adenocarcinoma; Meta = metastatic lung tumor; Large = large cell carcinoma; NA = not applicable; small = small cell carcinoma; ADESQ = adenosquamous cell carcinoma; SCC = squamous cell carcinoma.

between L/Ne and Pgp expression. The same results were obtained for mRNA level. The mean L/Nd of the Pgp mRNA low-expression group was significantly higher than that of the Pgp mRNA high-expression group ($P = 0.0127$) (Fig. 5A). The Pgp mRNA high-expression group had a higher L/Nwr than did the Pgp mRNA low-expression group ($P = 0.0825$) (Fig. 5B). No correlation was found between L/Ne and Pgp mRNA level. Uptake of tumor ^{99m}Tc-MIBI is associated with many factors, including direct mechanisms such as negative transmembrane potential and drug efflux pump and indirect mechanisms such as blood flow and capillary permeability. We considered L/Ne to be more affected by blood flow. In contrast, L/Nd and L/Nwr clearly reflected Pgp expression of intrinsic properties of the tumor.

It has been established that MRP belongs to the superfamily of ABC transmembrane transporter proteins and can act as a glutathione S-conjugate efflux pump (*7*–*9*). Recently, ^{99m}Tc-MIBI was shown to be a substrate for MRP in vitro (*22*). The abilities of Pgp and MRP transporters to wash out ^{99m}Tc-MIBI have been reported to be similar in cell lines, in spite of different suspected mechanisms of transport (*28*). However, cardiac muscle showed a low L/Nwr of ^{99m}Tc-MIBI and a low level of Pgp expression but a high level of MRP expression (*23*,*24*). The efficiencies of Pgp and MRP in transporting ^{99m}Tc-MIBI seem to be different in vivo. Likewise, in our clinical data, we did not observe any correlation between tumor accumulation or efflux of ^{99m}Tc-MIBI and the expression of MRP on protein level or mRNA level in lung cancer. We suppose that the discrepancy between in vitro and in vivo findings is closely associated with glutathione. The exact way in which glutathione is involved in MRP-mediated transport is unclear. One possibility is that glutathione forms transportable com-

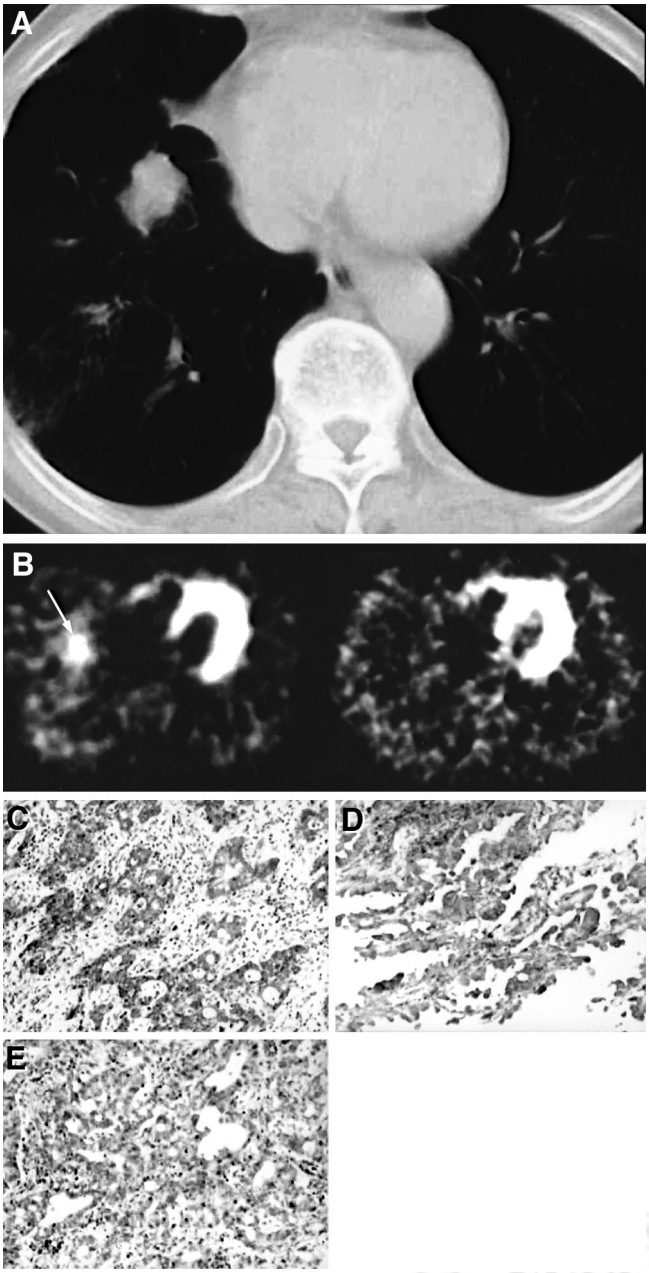

FIGURE 1. Patient 1, 73-y-old man with 2.8 × 2.8 cm lung adenocarcinoma. (A) CT scan shows nodule in right lung. (B) Early ^{99m}Tc-MIBI SPECT scan (left) shows intense uptake (arrow) of ^{99m}Tc-MIBI in tumor (L/Ne = 3.81). Delayed scan (right) shows faint ^{99m}Tc-MIBI uptake in tumor (L/Nd = 1.00), suggesting rapid washout of ^{99m}Tc-MIBI from tumor (L/Nwr = 73.8%). Immunohistochemistry (×200) reveals strong Pgp expression (C), strong MRP expression (D), and weak LRP expression (E) in corresponding tumor tissue.

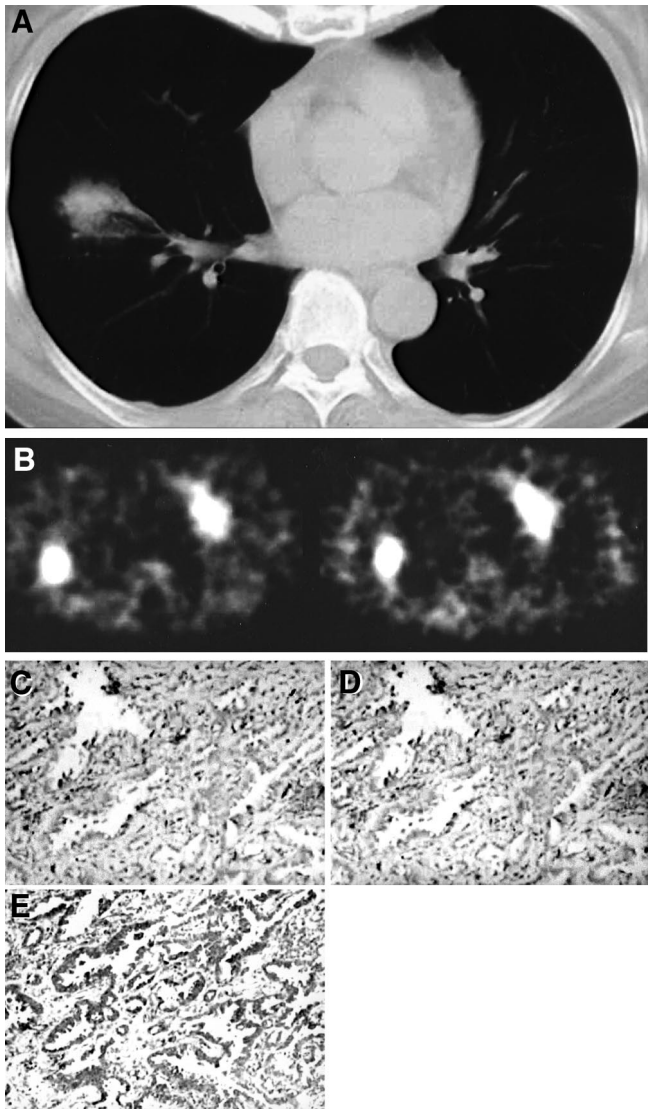

FIGURE 2. Patient 34, 68-y-old woman with 3.6 × 3.6 cm lung adenocarcinoma. (A) CT scan shows nodule in right lung. (B) Early ^{99m}Tc-MIBI SPECT scan (left) shows intense uptake of ^{99m}Tc-MIBI in tumor (L/Ne = 3.65). Delayed scan (right) also shows intense ^{99m}Tc-MIBI uptake in tumor (L/Nd = 5.17), suggesting slow washout of ^{99m}Tc-MIBI from tumor (L/Nwr = −41.6%). Immunohistochemistry (×200) reveals negative Pgp expression (C), negative MRP expression (D), and strong LRP expression (E) in corresponding tumor tissue.

plexes with cationic agents or reduces essential functional groups in the protein. Another possibility is that glutathione functions as a cotransporter to pump cationic drugs out of the cell by way of MRP (*29*). As observed in our data, these hypotheses suggest that glutathione and glutathione-S-transferase ([GST] an enzyme that catalyzes the glutathione conjugation reaction) are the essential functional components in glutathione-dependent MRP-mediated transport. Recently, depleted glutathione levels have been reported with reduced MRP-mediated MIBI transport (*30*). Increased glutathione levels have also been reported with resistance to alkylating agents and cisplatin (*31*). In addition, a significant correlation was found between resistance to doxorubicin and the expression of GST in 94 cases of non–small cell lung carcinoma (*32*). Therefore, although MIBI imaging of lung cancer is not associated with expression of MRP, MIBI imaging may be related to the levels of glutathione and

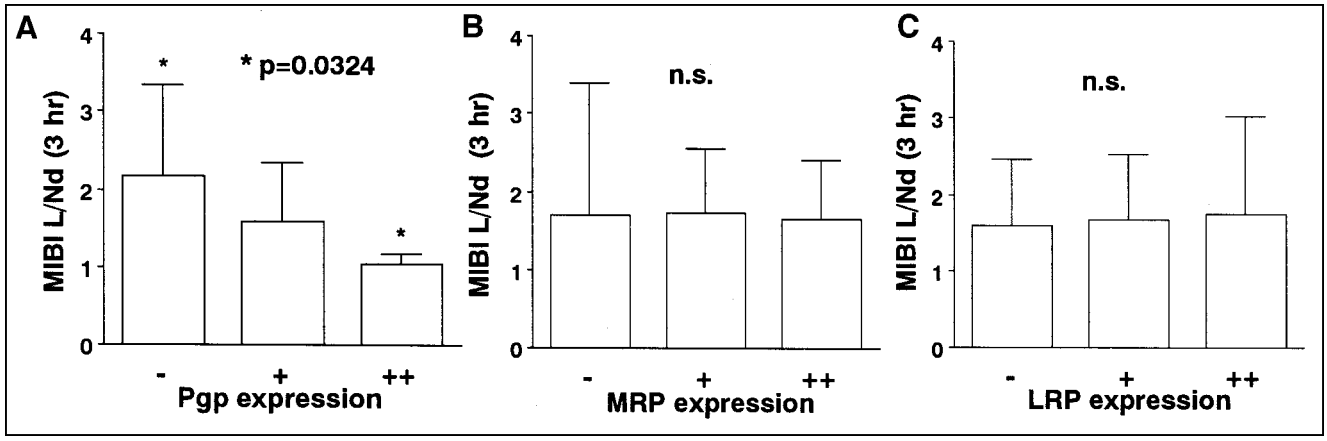

FIGURE 3. Relationship between expression of Pgp, MRP, or LRP and ^{99m}Tc-MIBI L/Nd in lung cancer. (A) L/Nd correlated inversely with density of Pgp expression. Statistically significant difference in L/Nd was found between Pgp (−) group and Pgp (++) group. (B) No significant difference (n.s.) in L/Nd was found among MRP (++), MRP (+), and MRP (−) groups. (C) No significant difference in L/Nd was found among LRP (++), LRP (+), and LRP (−) groups.

GST, which reflect the functionality of MRP-mediated transport.

LRP has been identified as the vault protein involved in nucleocytoplasmic transport (*11*). Recently, subcellular accumulation of drugs was found to be localized in the cytoplasm and minimally in the nuclei in LRP overexpression cells (*33*). Because of previous findings that increased cytoplasm concentration of the drug increases its contact with the membrane, we believed that efflux of the drug may be enhanced in LRP overexpression cells. However, we did not find a correlation between tumor accumulation or efflux of ^{99m}Tc-MIBI and expression of LRP. Subcellular accumulation of ^{99m}Tc-MIBI within the mitochondria and cytoplasm of cells has been reported to be based on transmembrane electric potentials (*34*). Therefore, efflux of ^{99m}Tc-MIBI was rarely affected by expression of LRP.

This study had limitations. First, some samples showed a discordance between MDR protein and mRNA levels, whereas Pgp expression on protein level (percentage of stained tumor cells) correlated significantly with mRNA expression ($r = 0.654$; $P = 0.0404$). This phenomenon may be explained by the biologic heterogeneity of tumors. Intratumoral heterogeneity of histologic features is widely recognized, having been most extensively studied in pulmonary carcinoma (*35*). In our study, the largest section in the middle of the tumor was stained for immunohistochemistry, because ROIs on ^{99m}Tc-MIBI SPECT were defined on the transaxial tomograms that showed the lesion's highest uptake to be in the middle of the tumor. RNA was prepared from a different area near the middle of the tumor. Second, the correlation of ^{99m}Tc-MIBI results with Pgp expression was obtained without taking into account MRP and LRP. Interaction between the 3 MDR proteins cannot be ruled out. Third, the results of this study address investigational more than clinical issues, because MDR is multifactorial. We did not calculate the correlation between response to

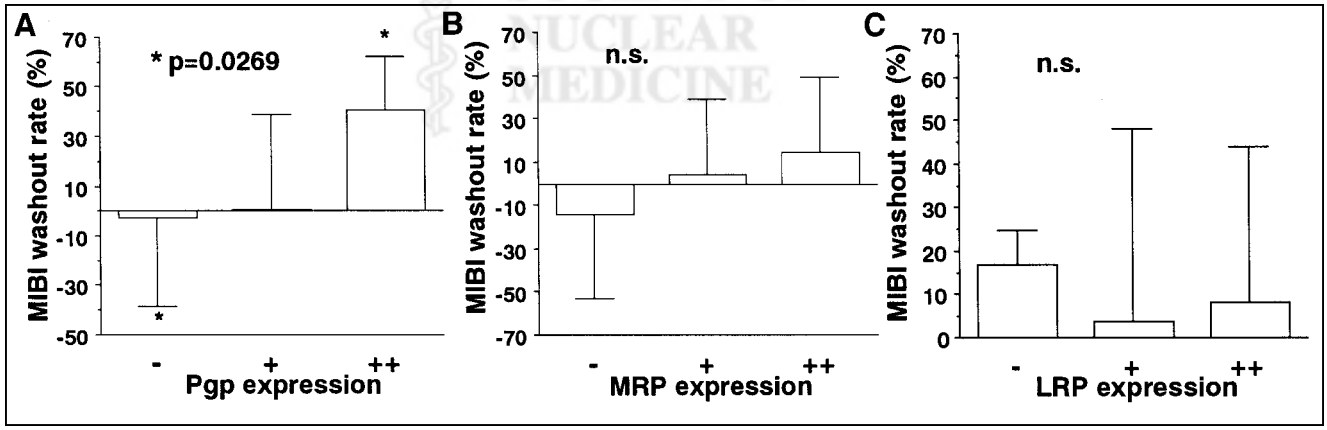

FIGURE 4. Relationship between expression of Pgp, MRP, or LRP and ^{99m}Tc-MIBI L/Nwr in lung cancer. (A) L/Nwr correlated with density of Pgp expression. Statistically significant difference in L/Nwr was found between Pgp (++) group and Pgp (−) group. (B) No significant difference (n.s.) in L/Nwr was found among MRP(++), MRP (+), and MRP (−) groups. (C) No significant difference in L/Nwr was found among LRP (++), LRP (+), and LRP (−) groups.

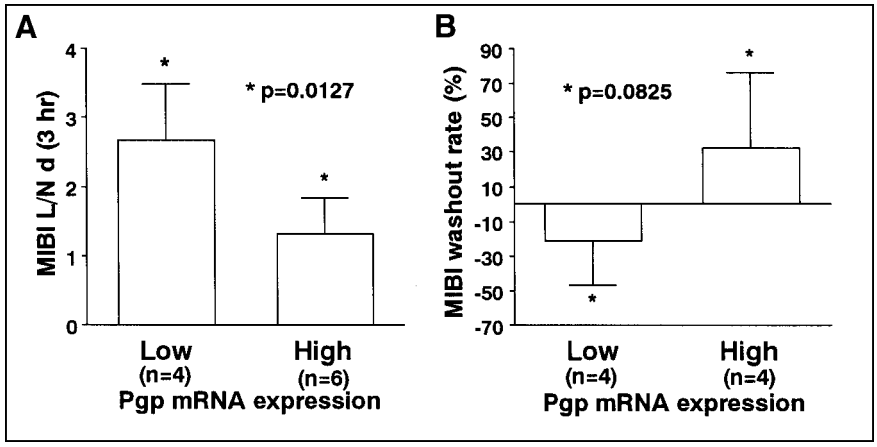

FIGURE 5. Relationship between Pgp mRNA expression and ^{99m}Tc-MIBI L/Nd or ^{99m}Tc-MIBI L/Nwr in lung cancer. (A) L/Nd correlated inversely with Pgp mRNA level. Statistically significant difference in L/Nd was found between Pgp mRNA low-expression group and Pgp mRNA high-expression group. (B) Statistical support was found toward a significant difference in L/Nwr between Pgp mRNA high-expression group and Pgp mRNA low-expression group.

chemotherapy and ^{99m}Tc-MIBI imaging because all patients underwent surgery. Furthermore, measurement of mRNA expression of MDR proteins does not necessarily provide information about the dynamic function of the drug efflux pump. MDR may be defined not by the number of MDR proteins on tumor cells but by the functional transport capacity of drug efflux pumps. Clearly, additional clinical study is essential.

CONCLUSION

In this preliminary study, we searched for correlations between both tumor uptake and clearance of ^{99m}Tc-MIBI with an MDR phenotype (Pgp, MRP, and LRP) on protein and mRNA levels. A close connection exists between ^{99m}Tc-MIBI imaging of lung cancer and expression of Pgp. The L/Nd and L/Nwr of ^{99m}Tc-MIBI are useful for noninvasively detecting the expression of Pgp in lung cancer. ^{99m}Tc-MIBI may not be useful in identifying the expression of MRP or LRP.

ACKNOWLEDGMENTS

This study was supported by grants for project research (H00-2 and A99-1) from the High-Technology Center of Kanazawa Medical University; a grant-in-aid for cancer research (12-4) from the Ministry of Health and Welfare, Japan; and a grant-in-aid for scientific research (13670192) from the Ministry of Education, Science, and Culture, Japan.

REFERENCES

1. Volm M, Mattern J. Detection of multiple mechanisms in untreated human lung cancer. *Onkologie.* 1993;16:189–194.
2. Oberli-Schrammli AE, Joncourt F, Stadler M, et al. Parallel assessment of glutathione-based detoxifying enzymes, O6-alkylguanine-DNA alkyltransferase and P-glycoprotein as indicators of drug resistance in tumor and normal lung of patients with lung cancer. *Int J Cancer.* 1994;59:629–636.
3. Volm M. Multidrug resistance and its reversal. *Anticancer Res.* 1998;18:2905–2918.
4. Scagliotti GV, Novello S, Selvaggi G. Multidrug resistance in non-small-cell lung cancer. *Ann Oncol.* 1999;10(suppl 5):S83–S86.
5. Danks M, Yalowich J, Beck W. Atypical multiple drug resistance in a human leukemic cell line selected for resistance to teniposide (VM-26). *Cancer Res.* 1987;47:1297–1301.
6. Gottesman MM. How cancer cells evade chemotherapy. *Cancer Res.* 1993;53:747–754.
7. Leier I, Jedlitschky G, Buchholz U, et al. The MRP gene encodes an ATP-dependent export pump for leukotriene C4 and structurally related conjugates. *J Biol Chem.* 1994;269:27807–27810.
8. Versantvoort CH, Broxterman HJ, Bagrij T, Scheper RJ, Twentyman PR. Regulation by glutathione of drug transport in multidrug-resistant human lung cell lines overexpressing multidrug resistant-associated protein. *Br J Cancer.* 1995;72:82–89.
9. Higgins CF. ABC transporters: from microorganisms to man. *Annu Rev Cell Biol.* 1992;8:67–113.
10. Cole SP, Bhardwaj G, Gerlach JH, et al. Overexpression of a transporter gene in a multidrug-resistance human lung cancer cell line. *Science.* 1992;258:1650–1654.
11. Scheffer GL, Wijngaard PL, Flens MJ, et al. The drug resistance-related protein LRP is the human major vault protein. *Nat Med.* 1995;6:578–582.
12. Abrams MJ, Davison A, Jones AG, Costello C. Synthesis and characterization of Hexakis (alkyl isocyanide) and hexakis (aryl isocyanide) complexes of technetium (I). *Inorg Chem.* 1983;22:2798–2800.
13. Wackers MJ, Berman DS, Maddahi J, et al. Technetium-99m hexakis 2-methoxy-isobutylisonitrile: human biodistribution, dosimetry, safety and preliminary comparison to thallium-201 for myocardial perfusion imaging. *J Nucl Med.* 1989;30:301–311.
14. Hassan IM, Sahweil A, Constantinides C, et al. Uptake and kinetics of Tc-99m hexakis 2-methoxy isobutyl isonitrile in benign and malignant lesions in the lungs. *Clin Nucl Med.* 1989;14:333–340.
15. Aktolun C, Bayhan H, Kir M. Clinical experience with Tc-99m MIBI imaging in patients with malignant tumors: preliminary results and comparison with Tl-201. *Clin Nucl Med.* 1992;17:171–176.
16. Kao C-H, Wang S-J, Lin W-Y, et al. Differentiation of single solid lesions in the lungs by means of single-photon emission tomography with technetium-99m methoxyisobutylisonitrile. *Eur J Nucl Med.* 1993;20:249–254.
17. Wang H, Maurea S, Mainolfi C, et al. Tc-99m MIBI scintigraphy in patients with lung cancer: comparison with CT and fluorine-18 FDG PET imaging. *Clin Nucl Med.* 1997;22:243–249.
18. Piwnica-Worms D, Chiu ML, Budding M, Kronauge JF, Kramer RA, Croop JM. Functional imaging of multidrug resistance P-glycoprotein with an organotechnetium complex. *Cancer Res.* 1993;53:977–984.
19. Kostakoglu L, Elahi N, Kiratli P, et al. Clinical validation of the influence of p-glycoprotein on technetium-99m-sestamibi uptake in malignant tumors. *J Nucl Med.* 1997;38:1003–1008.
20. Kostakoglu L, Kiratli P, Ruacan S, et al. Association of tumor wash-out rates and accumulation of ^{99m}Tc-MIBI with the expression of p-glycoprotein in lung cancer. *J Nucl Med.* 1998;39:228–234.
21. Del Vecchio S, Ciarmiello A, Potena MI, et al. In vivo detection of multi-drug resistant (MDR1) phenotype by technetium-99m-sestamibi scan in untreated breast cancer patients. *Eur J Nucl Med.* 1997;24:150–159.
22. Hendrikse NH, Franssen EJ, van der Graaf WT, et al. ^{99m}Tc-sestamibi is a substrate for P-glycoprotein and the multidrug resistance associated protein. *Br J Cancer.* 1998;77:353–358.

23. Fojo AT, Ueda K, Slamon DJ, et al. Expression of a multidrug-resistance gene in human tumors and tissues. *Proc Natl Acad Sci USA.* 1987;84:265–269.
24. Flens MJ, Zaman GJ, van der Valk P, et al. Tissue distribution of the multidrug resistance protein. *Am J Pathol.* 1996;148:1237–1247.
25. Izquierdo MA, Scheffer GL, Flens MJ, et al. Broad distribution of the multidrug resistance-related vault lung resistance protein in normal human tissues and tumors. *Am J Pathol.* 1996;148:877–887.
26. Livak KJ, Flood SJ, Marmaro J, Giusti W, Deetz K. Oligonucleotides with fluorescent dyes at opposite ends provide a quenched probe system useful for detecting PCR product and nucleic acid hybridization. *PCR Methods Appl.* 1995;4:357–362.
27. Higuchi R, Fockler C, Dollinger G, Watson R. Kinetic PCR analysis: real-time monitoring of DNA amplification reactions. *Biotechnology.* 1993;11:1026–1030.
28. Vergote J, Moretti JL, de Vries EG, Garnier-Suillerot A. Comparison of the kinetics of active efflux of ^{99m}Tc-MIBI in cells with P-glycoprotein-mediated and multidrug-resistance protein-associated multidrug-resistance phenotypes. *Eur J Biochem.* 1998;252:140–146.
29. Hendrikse NH, Franssen EJ, van der Graaf WT, Vaalburg W, de Vries EG. Visualization of multidrug resistance in vivo. *Eur J Nucl Med.* 1999;26:283–293.
30. Moretti JL, Cordobes MD, Starzec A, et al. Involvement of glutathione in loss of technetium-99m-MIBI accumulation related to membrane MDR protein expression in tumor cells. *J Nucl Med.* 1998;39:1214–1218.
31. Lewis AD, Hichson ID, Robson CN, et al. Amplification and increased expression of alpha class glutathione S-transferase encoding genes associated with resistance to nitrogen mustards. *Proc Natl Acad Sci USA.* 1988;85:8511–8517.
32. Volm M, Rittgen W. Cellular predictive factors for the drug response of lung cancer. *Anticancer Res.* 2000;20:3449–3458.
33. Cheng SH, Lam W, Lee ASK, Fung KP, Wu RS, Fong WF. Low-level doxorubicin resistance in benzo[a]pyrene-treated KB-3-1 cells is associated with increased LRP expression and altered subcellular drug distribution. *Toxicol Appl Pharmacol.* 2000;164:134–142.
34. Piwnica-Worms D, Kronauge JF, Chiu ML. Uptake and retention of hexakis (2-methoxyisobutyl isonitrile) technetium(I) in cultured chick myocardial cells: mitochondrial and plasma membrane potential dependence. *Circulation.* 1990; 82:1826–1838.
35. Dunnill MS, Gatter KC. Cellular heterogeneity in lung cancer. *Histopathology.* 1986;10:461–475.